First publ. in: Journal of Chemical Physics 102 (1995), 12, pp. 5082-5087

Grain size control in polycrystalline colloidal solids

Thomas Palberg, Wolfgang Mönch, Jürgen Schwarz, and Paul Leiderer
Universität Konstanz, Fakultät f. Physik, D-78434 Konstanz, Germany

(Received 15 September 1994; accepted 5 December 1994)

Recent experiments on the static and dynamic properties of polycrystalline colloidal solids show a pronounced influence of morphological details. Here we investigate several possibilities to vary systematically one key morphological parameter, namely the average crystallite radius r_c of polycrystalline solids. We report measurements of r_c as observed by microscopy in well-characterized Yukawa model suspensions. The pair energy of interaction is systematically varied through precise experimental adjustment of the suspension parameters packing fraction Φ, number of ionic surface groups N, and concentration of screening ions c. The average size is found to systematically decrease with increasing interaction. At fixed suspension parameters we performed solidification under shear, i.e., in the presence of alternating electric fields. We report preliminary results in dependence on both the electric field strength and frequency. The grain size increases with increasing shear rates. It shows a complex behavior as a function of the frequency and the wave form of the applied field. Qualitative explanations are discussed and a first application is presented.

I. INTRODUCTION

Monodisperse colloidal particles suspended in viscous fluids spontaneously form so-called colloidal fluids or solids, if the experimentally variable interaction between the particles is strong enough.[1–3] These highly correlated systems became widely recognized as model systems to study very general phenomena of condensed matter physics like phase transitions,[4] transport phenomena,[5] or elastic behavior.[3,6] For charged particles these properties are first of all related to the parameters of the Yukawa or screened Coulomb interaction, namely the packing fraction of particles Φ, their surface potential Ψ_0, and the concentration of screening ions c. These parameters can be experimentally varied at constant temperature T with high precision. However, as for atomic systems the equilibrium properties of colloidal solids furthermore show a pronounced dependence on the sample morphology. For example, it was observed that polycrystalline colloidal material shows an increase of the tracer diffusion coefficient over several orders of magnitude when the grain size is decreased from some millimeters to 50 μm.[7] At the same time the shear modulus of the system shows significant deviations towards values higher than expected.[8] These effects reveal a strong analogy to the size dependences in nanocrystalline atomic materials, where grain boundary diffusion is the predominant transport mechanism and a transition from homogeneous distribution of elastic strains to a homogeneous distribution of stresses is observed with decreasing grain size. Also other morphological details, like form and orientation of crystallites, grain boundary structure, twinning, etc., may strongly influence the material properties.[9]

The typical lattice spacings of colloidal solids are on the order of the wavelength of visible light. The presence of the viscous suspending medium leads to a convergence of time scales which are widely separated for atomic systems. Both structure and dynamics are therefore easily accessible by light scattering methods, while the morphology is well observable also by microscopy.[4,10] Studies on these model systems are particularly interesting because the dominating parameters may be separated. This implies that, for example, the dependence of the resulting morphology on the degree of undercooling may be discriminated from the influence of a shear flow. Most often there are only negligible density differences between metastable melt and solid even during solidification. (For some important exceptions, however see, e.g., Refs. 4 and 11.) Moreover the experiments can be performed at constant temperature with the suspending fluid acting as a heat bath. Thus in most cases also the effects caused by heat and mass transport may be excluded. Colloidal solids thus provide a unique chance to systematically investigate morphological influences on the properties of solids on a microscopic level, with high temporal resolution and under well-defined conditions.

The basis of such studies would obviously be formed by techniques to reproducibly prepare selected morphologies and by an independent access to their variation. It has been reported that for Yukawa systems crystallizing from the undercooled melt the suspension parameters determine, e.g., the grain size via the nucleation rate density.[12,13] After complete solidification shear processing may lead to strong changes within the sample,[9,14] even to shear melting.[6,15] Crystallization under oscillatory mechanical shear has been reported to lead to the formation of twinned oriented wall crystals, which show checkerboardlike twinning patterns.[3,16] These studies already provided valuable information about some aspects of freezing transitions with and without applied shear. Despite these promising results we are, however, still far from having a consistent microscopic picture of morphological influences on the properties of solids. A comprehensive understanding of this problem would have important implications in a variety of fields ranging from the processing of dense dispersions or polymer melts to rheocasting or convection processes in the earth.

We here report a first systematic study on the solidification of metastable melts of charged latex spheres (i) without applied shear under variation of the packing fraction, the

TABLE I. Experimental parameters of the suspensions under study. The hydrodynamic radii a_h were determined by dynamic light scattering. The suspension parameters were in all cases adjusted using the technique of continuous de-ionization (Ref. 20) under the control of static light scattering, conductivity, and conductivity titrations. The uncertainties in Φ, c, and N are less than 1%, 2%, and 5%, respectively.

Sample	Radius	Packing fraction	Salt concentration	Surface group number
	a_h (nm)	Φ	c (μmol ℓ^{-1})	N
FEP-7	39	0.0018–0.0157	0–7	500–1265
D-109	51	0.0035	0	950

strength and the range of the Yukawa interaction and (ii) at constant suspension parameters in the presence of shearing electric fields. After a short introduction of the substances and experimental techniques we present detailed material on the accessible range of crystallite sizes with and without application of shear. We also study the differences caused by variations of the shear parameters and suggest a qualitative explanation for the observed suppression of homogeneous nucleation in the presence of shearing fields. Then a first example of a complex morphology prepared by solidification under shear is presented.

II. EXPERIMENT

Two kinds of particles were used in this study which have been characterized extensively by light scattering and other methods.[17–19] In particular, the $\Phi-c$ phase diagram for the D-109 system and the $N-c$ phase diagram for the FEP-7 system have been determined before in independent experiments. The main particle data are listed in Table I together with the respective experimental suspension parameters.

D-109 samples were prepared from commercially available, aqueous suspensions of polystyrene latex spheres each carrying a fixed number of ionizable surface groups FEP-7 was kindly provided by the group of V. Degiorgio (Pavia, I) and were originally manufactured by Montefluos, Turin, Italy. Their charge is due to some thousand physisorbed strongly hydrophobic surfactant molecules. It can be varied by controlled desorption under treatment with ion exchange resin (MB1, Serva, Germany). Since the refractive index of the perfluorinated particles is close to that of water, even at elevated packing fractions Φ transparent samples may be prepared. A recently reported advanced de-ionization technique was used to reproducibly adjust the experimental suspension parameters packing fraction Φ and concentration of screening ions c, and also to control the number of surfactant groups N of the FEP-7 particles.[20] The suspension is pumped peristaltically through a Teflon tubing system connecting (i) the ion exchange chamber, (ii) reservoirs under inert gas atmosphere to add $p.a$ grade salt solutions (Merck, Germany) or further suspension, (iii) the observation cell, (iv) a cell for static light scattering or transmission experiments, and (v) a conductivity measurement (WTW, Germany). The latter experiments facilitate an *in situ* control of Φ and c. Under salt free conditions N is determined via a conductivity-group number calibration curve. During the actual crystallization experiments the ion exchange chamber is bypassed and great care is taken to assure stable experimental conditions on a typical time scale of a few hours. Uncertainties in the experimental parameters are found to be less than 1%, 2%, and 5% for Φ, c, and N, respectively.

At the chosen experimental parameters the equilibrium phase of both suspensions is body centered cubic. However, during preparation the sample is shear molten and is left as a metastable melt, once the flow is stopped by electromagnetic valves. It then readily crystallizes with solidification front velocities in the 0.1–10 μm s^{-1} range depending on the suspension parameters. The observation cells of rectangular cross section (1–5 mm$\times$10 mm, Rank, UK) contain an electrode arrangement to apply a homogeneous electric field. Both maximum field strengths reaching $E\approx 200$ V cm^{-1} and frequencies 0.05 Hz $<f<50$ Hz are controlled with accuracies better than 1%. In addition to dc fields sinusoidal and square wave fields may be applied to the cell which is closed against the preparation tubing system during measurements. Upon application of an electric field one observes a nearly parabolic shear flow in the center plane due to electroosmotic backflow along the cell walls.[21] The particles move at velocities being the sum of their electrophoretic velocity (where for highly charged polystyrene particles at de-ionized conditions the mobility typically is on the order of $\mu\approx 10$ μm s^{-1}/V cm^{-1})[21] and the underlying velocity profile within the suspending medium. The shear rates decrease linearily towards the cell center and are proportional to the applied field strength.

Solidification with or without applied shear is monitored on the stage of a polarization microscope (Labolux 12, Leitz, Germany). Video frames are recorded and further processed by image analysis (Optimas, Stemmer, Germany). Homogeneously nucleated crystals growing in the bulk melt prevail with and without applied shear. During growth their shape is a rounded polyeder. Upon intersection a three-dimensional mosaic of irregularily faceted crystallites is formed. In the unsheared case an oriented monolithic wall crystal grows in addition, if the suspension parameters are close to those at melting. Its growth is stopped upon intersection with bulk crystals. In the case of solidification under shear homogeneous nucleation is restricted to the volume in the cell center. This polycrystalline plug is lubricated by sliding layers which directly transform into an oriented monolithic crystal, once the shear flow is stopped. Thus in both cases only a core of polycrystalline material is formed. Its thickness may however become quite large, depending on the employed cell geometry. The orientational distribution of crystallites in the core was checked by konoscopy to be random.

In this study we restrict ourselves to the grain size analysis of frames taken after complete solidification. The shape of intersected crystallites still is approximately spherical and the half geometric mean of the longest and shortest diameter is taken as a measure of the crystallite radius $r_c=0.5$ $(ab)^{1/2}$. The distribution of r_c is strongly peaked and can be approximated in the unsheared case by a Gaussian with a full width at half-height of typically less than 20% of the mean crystallite radius averaged over 100–1000 crystallites.

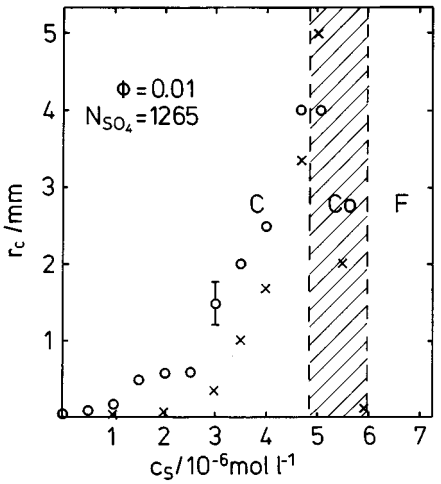

FIG. 1. Average crystallite dimensions as a function of the salt concentration c as observed after solidification without shear in a suspension of FEP-7 particles with fixed packing fraction of $\Phi=0.01$ and a number of ionizable surface groups of $N=1265$. The symbols are: (○) radii of homogeneously nucleated crystallites; (×) thickness of the heterogeneously nucleated wall crystal. The hatched area denotes the coexistence regime (CO) between body centered cubic crystalline (C) and fluid phase (F).

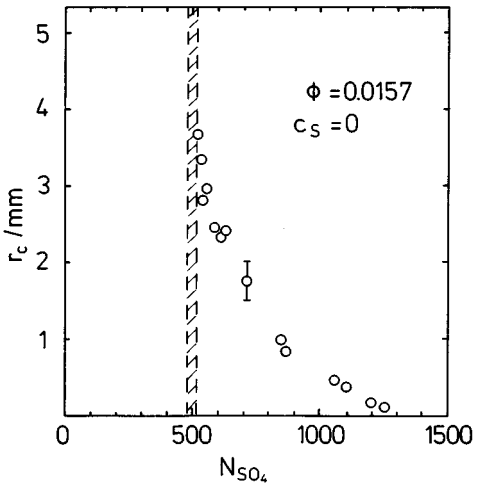

FIG. 3. Average crystallite dimensions as a function of the number of ionizable surface groups N as observed after solidification without shear in a suspension of FEP-7 particles with fixed salt concentration of $c=0$ and packing fraction of $\Phi=0.01$. Symbols as in Fig. 1.

III. RESULTS

We first systematically investigated the possibilities of size control via variations of the suspension parameters salt concentration c, packing fraction Φ, and the number of ionizable surface groups N. Using the FEP-7 system, three series of experiments were performed. In each we kept two parameters constant, while varying the third one. Each series consisted of up to ten runs and excellent reproducibility was observed in r_c which differed from run to run by less than 5%. The results are presented in Figs. 1–3. In all three cases the largest crystals are grown close to the experimentally observed phase boundaries, respectively, in the coexistence regimes. The crystallite radii decrease with increasing strength of interaction, i.e., with increasing packing fraction Φ or number of surfactant groups N and with decreasing salt concentration c. For the salt concentration dependent measurements also the thickness of the wall crystal is included in Fig. 1. It starts growing from a number of oriented particle layers adjacent to the cell wall immediately after the shear flow is interrupted. Its growth is terminated upon intersection with bulk nucleated crystals. Therefore its increasing thickness indicates the drastic decrease in rate densities for homogeneous nucleation, as the phase boundary is approached. At coexistence the wall crystal thickness is larger than r_c and goes through a maximum c reflecting the decreasing volume of solidifying material with increasing salt concentration. Such crystals have already been used as reference samples in the study of tracer diffusion processes.[7]

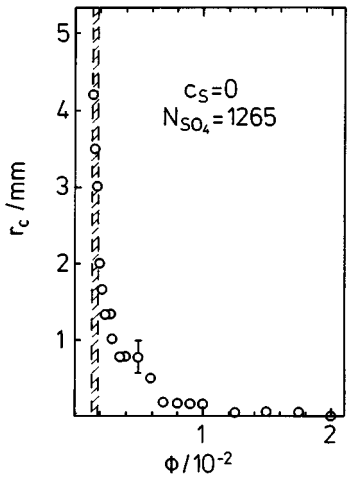

FIG. 2. Average crystallite dimensions as a function of the packing fraction Φ as observed after solidification without shear in a suspension of FEP-7 particles with fixed salt concentration of $c=0$ and number of ionizable surface groups of $N=1265$. Symbols as in Fig. 1.

The data clearly show that the grain size may be varied over several orders of magnitude by altering the suspension parameters. Close to the phase boundary very large crystals are observed and at large undercooling extremely small crystallites are formed. The underlying mechanism is the control of the nucleation rate density J. Detailed investigations performed on the D-109 system will be reported elsewhere.[22] We here just note that J scales according to classical nucleation theory as $J=J_0\exp(-\Delta G^*/k_BT)$, where ΔG^* is the free energy barrier to form a critical nucleus, k_B is the Boltzmann constant, and T the temperature. The prefactor J_0, however is not constant as observed in atomic systems but shows an exponential dependence on the quantity $\Pi=\rho V(r)$, where $\rho=3\Phi/4\pi\, a^3$ is the density of particles with radius a and $V(r)$ is the pair energy of interaction. In the present study the values for J as calculated from the extended Avrami model of Aastuen *et al.*[13] reach $J=10^{15}$ $\mathrm{m^3\,s^{-1}}$ under conditions of strongest interaction.

In order to introduce systematic grain size variations without altering the interaction we performed additional solidification experiments at constant suspension parameters, but in the presence of variable shear flows. Here we used the

(a)

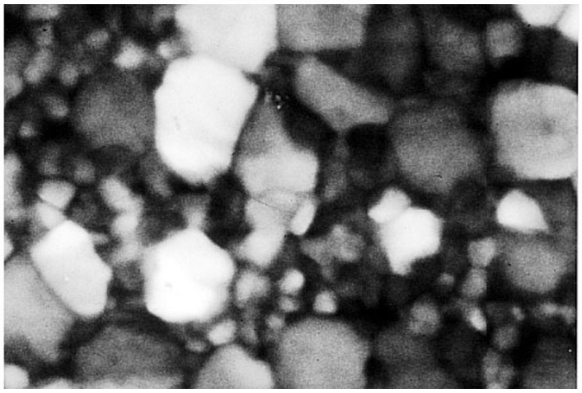

(b)

FIG. 4. Polarization microscopical pictures of a completely solidified D-109 suspension at a packing fraction of $\Phi=0.0035$ and no added salt. (a) After crystallization without application of shear. Note the fairly homogeneous size of the crystallites. The size distribution is strongly peaked with an average grain size of 30 μm; (b) after crystallization in the presence of a shearing electric field, for details of the time dependent amplitude see the text. Note the bimodal size distribution of large crystallites embedded in a matrix of smaller ones. Field of view 400×600 μm in both cases.

D109 system at both fixed packing fraction and salt concentration. This corresponds to an average crystallite radius of $r_c=15$ μm in the unsheared case. The extremely tiny crystallites are hardly visible to the naked eye but can still to be resolved under 500 times magnification. We show an example in Fig. 4(a), taken from a completely deionized D-109 sample at a packing fraction of $\Phi=0.0035$. For the same suspension the long time self-diffusion coefficient was recently determined to be only one order of magnitude smaller than that of the metastable melt,[7] which was the first documentation of grain boundary diffusion within a nanocrystalline colloidal solid. Indeed a crystallite of only some 20 μm radius contains only as few as 10^4–10^5 particles and the estimated fraction of grain boundaries may well reach 10% of the sample volume.

The samples were first shear molten, then, still under flow, an alternating electric field was applied, and finally the cell was closed against the tubing system by the electromagnetic valves. Both sine and square wave fields of variable field strength and frequency were used. In most cases we observed the following scenario. Solidification starts from the cell center, where the shear rates are lowest. The size of crystallites formed in this region is fairly independent of their position, but highly sensitive to the overall shear parameters. A polycrystalline plug is formed which is pushed forward and backward in a pistonlike fashion without showing internal plastic flow. It is lubricated against the wall by thin regions of noncrystalline material. This configuration is stationary and the structure of the lubricating regions was determined by static light scattering to consist of hexagonal sliding layers. Such structure meanwhile is well documented for a large number of systems and shearing conditions from the interpretation of light and neutron scattering data[23–25] and from computer simulations.[26] After termination of shear the latter region solidifies very rapidly and directly into an oriented monolithic wall crystal of bcc structure.

This interesting solidification behavior is currently not well understood. It is qualitatively different from the case of mechanical oscillatory shear, where solidification starting from the cell wall was reported and interpreted in terms of a flow instability.[3,16] Plug flows of polycrystalline material with lubrication by either shear molten material or sliding layers were observed under steady mechanical flow through tubes of rectangular shape.[8,27] While in most cases of steady shearing the sliding layers fill the whole of the sample cell, very little is known about the resulting morphologies after cessation of shear. The main difference as compared to the case of mechanically induced shear flows and to the unsheared case, however, is the presence of the electro-osmotic counterflows in the vicinity of the cell walls.[21] We therefore do not have sticking conditions at the cell wall and heterogeneous nuclei are unstable. Instead of nucleation and growth of a wall nucleated crystal against a metastable melt of fluid order[13,16,17] we observe an instantaneous registering of hexagonal sliding layers to form the (110) planes of the body centered cubic wall crystal. In fact, both polarization microscopical analysis and the time development of the Bragg scattering pattern show a direct transition from the sliding layer state to the oriented monolithic crystal.

Obviously, complex composite morphologies are formed under these conditions. The amount of monolithic material, however, may be kept low by choosing a suitable cell geometry and we now return to the question of grain size control within the polycrystalline core region. In all cases crystal growth is much less affected than nucleation. The typical growth velocities are still on the order of some 5–7 μm s^{-1} as compared to 10 μm s^{-1} in the unsheared case, while the nucleation rates are decreased by several orders of magnitude. In Fig. 5 we show that at a constant frequency of $f=1$ Hz for both wave forms the grain size strongly increases with increasing field strength. The increase is less pronounced for the sine wave case. After solidification under shear the distribution of crystallite sizes is slightly broadened as compared to the unsheared case and it shows a significantly asymmetric shape. Under fixed field strength of $E=75$ V cm qualitative differences in the frequency dependence of the crystallite radii are observed for the two wave forms. In Fig. 6 we show that the application of steady shear ($f=0$ Hz in the square wave case) leads to the formation of very large crystallites. Upon increasing the frequency r_c decreases to reach a plateau value for $f>15$ Hz, which is still signifi-

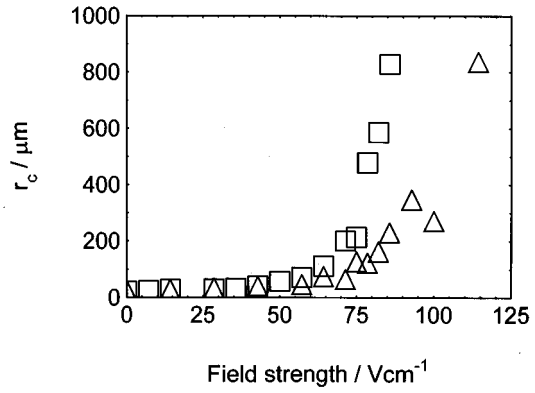

FIG. 5. Average crystallite radii as a function of the amplitude E of the shearing electric field of frequency $f=0.5$ Hz applied during solidification of a D-109 suspension at a packing fraction of $\Phi=0.0035$ and no added salt. The symbols denote: (△) sine wave field; (□) square wave field.

cantly larger than in the unsheared case. In the case of sine wave fields the radii increase drastically as the frequency is marginally increased above zero. At 1 Hz a maximum value is reached. The radii decrease again to reach the same plateau value as in the square wave case. We conclude that the differences in the field strength dependence depicted in Fig. 5 is due to the qualitatively different frequency behavior shown in Fig. 6. In fact, if the experiments are performed at fixed frequencies above 20 Hz the field-dependent radii for both wave forms coincide within the experimental error.

To qualitatively capture this behavior, we propose a suppression of homogeneous nucleation through a disruption of subcritical nuclei and the disturbance of diffusive relaxation into nuclei of crystalline structure while the suspension is sheared. The maximum distance x a particle is carried away from its original neighborhood is to a first approximation proportional to the field strength via the amplitude of the parabolic electro-osmotic velocity profile.[17] At fully developed electro-osmotic profiles the shear rate and therefore also x increase linearly with E and with the distance y from the cell center. Moreover x is proportional to the inverse of the alternation frequency f of a square wave field. Assuming

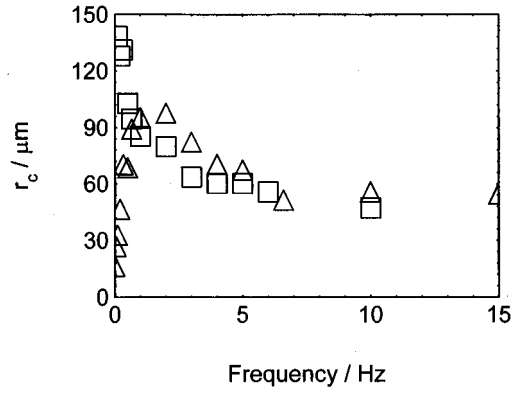

FIG. 6. Average crystallite radii as a function of the frequency f of the shearing electric field of amplitude $E=55$ V/cm^{-1} applied during solidification of a D-109 suspension. Suspension parameters and symbols as in Fig. 5.

diffusional transport of particles back to the forming nucleus the nucleation rates under shear J_{shear} are expected to be proportional to $J_{\text{shear}}\sim JD/x^2=JDf^2/y^2E^2$, where J is the nucleation rate without shear. Fits of this expression using the long-time self-diffusion coefficient D determined for the unsheared metastable melt[7] to the square wave data gave a rough qualitative agreement for the dependence on the field strength and the frequency.

Although this qualitatively supports the proposed model, a number of problems remain. The measured average crsytallite radii do not tend to the value determined without shear for large applied fields. They rather saturate at a somewhat larger value. Moreover the model does not explain the difference between the two different wave forms. A possible solution is the assumption of an unsteady amplitude of the shear rate. During the periods of sign reversal of the electric field the suspension is relatively undisturbed until the osmotic velocity profile is re-established. It therefore seems plausible that nucleation proceeds less disturbed during these periods. They are much longer in the case of sine wave fields and are absent in the case of steady shear. This might qualitatively explain the differences in the frequency dependence observed for the two wave forms.

A much stronger objection might be raised concerning the proposed position dependence of the nucleation rates and correspondingly the spatial variation of crystallite size. No significant decrease in the grain size towards the cell center was observed in any of the nucleation scenarios. Therefore we suspect either a strong influence of the flow profile due to already nucleated crystals as has been observed in the case of electrophoresis measurements on crystalline suspensions[21] or incompletely developed electro-osmotic flow profiles. Recent detailed investigations of the latter in dependence on the applied frequency showed strong deviations from the steady field case with parabolic flow profile.[28] More systematic data including experimental determination of flow velocities are currently recorded to clarify this important issue.

We have shown that the solidification in the presence of alternating electric fields facilitates variations in the crystallite size of more than an order of magnitude. Concerning experiments on the properties of polycrystalline colloidal solids, this provides a valuable tool to systematically discriminate between the influences of the suspension parameters and those due to the sample morphology. Our studies differed from previous ones in the kind of applied shearing field. The use of electric fields limits the range of applicability to ionic solutions and suspensions. It is nevertheless obvious, that the proposed mechanism of shear suppression of nucleation bears very general implications for the freezing transition in the presence of shearing fields of whatever nature. One direct advantage of our approach is the time scale of the suspension response. Although it takes some milliseconds for the electro-osmotic profile to establish, no long-lasting inertial effects are present, which would lead to continuation of shear upon reversal or interruption of the electric field. This offers the possibility of applying a well-defined succession of shear conditions.

While it is well known that solids of complex morphology often also show complex elastic and plastic behavior at

present no microscopic theory is available to describe the influences of grain size *distributions*. In the present study we observed peaked distributions of fairly symmetric shape in the unsheared case. Asymmetric distributions were observed after solidification under shear. Further variations in the size distribution may be introduced using slightly modified shear conditions. Reduction of shear flow after a first period of shear-slowed nucleation leads to a sudden drastic increase in the nucleation rates. After a short period of time the shearing is continued at the original value of the electric field and the nucleation rates again are very small. A bimodal size distribution results and we show a representative example in Fig. 4(b). Large crystals are embedded in a matrix of smaller ones. Note in particular, that both grain sizes are much larger than in the unsheared case shown in Fig. 4(a). Preliminary measurements of the shear modulus of this sample indicate that its value is significantly lowered as compared to the shear modulus measured on the same sample after solidification without shear.

IV. CONCLUSIONS

In this study we have presented systematic measurements on the grain size in polycrystalline colloidal solids in dependence of various suspension parameters. In addition we observed strong influences of alternating electric fields on the solidification process via a suppression of nucleation under shear. The proposed qualitative model captures some of the essentials of the observed freezing transition in the presence of shear. The detailed explanation, however remains a challenge. The data presented were by no means comprehensive, they nevertheless demonstrated new ways of controlling the morphology of polycrystalline colloidal solids. In turn these materials of controlled average grain size and size distribution provide an excellent possibility to investigate the influences of morphological parameters on the properties of polycrystalline solids and may substantially aid the development of the corresponding microscopic understanding.

ACKNOWLEDGMENTS

The authors would like to thank M. Würth and H. Löwen for numerous critical discussions on the issue of the nucleation mechanisms. We are further indepted to V. Degiorgio, R. Piazza and T. Bellini for their introduction into the world of FEP-7. This part of the present study was financially supported by the DAAD vigoni program. Financial support of the Deutsche Forschungs Gemeinschaft is also gratefully acknowledged.

[1] P. N. Pusey in *Liquids, Freezing and the Glass Transition*, edited by J. P. Hansen, D. Levesque, and J. Zinn-Justin, 51st ed. Ecole d'ete, Les Houches, 1989 (Elsevier, Amsterdam, 1991), p. 637.
[2] Atelier d'Hiver sur les Cristaux Colloidaux; Les Houches 1985: J. Phys. C**3**, 46 (1985).
[3] P. M. Chaikin, J. M. diMeglio, W. Dozier, H. M. Lindsay, and D. A. Weitz, in *Physics of Complex and Supramolecular Fluids*, edited by S. A. Safran and N. A. Clark (Wiley, New York, 1987), p. 65.
[4] B. J. Ackerson (Ed.), Phase Transitions **21**, 1–323 (1990).
[5] R. Klein, in *Structure and Dynamics of Strongly interacting Colloids and Supramolecular Aggregates*, edited by S.-H. Chen, J. S. Huang, and P. Tartaglia NATO-ASI Vol. **369** (Kluwer, Dordrecht, 1992), pp. 39.
[6] M. O. Robbins, K. Kremer, and G. S. Grest, J. Chem. Phys. **88**, 3286 (1988).
[7] R. Simon, T. Palberg, and P. Leiderer, J. Chem. Phys. **99**, 3030 (1993).
[8] T. Palberg and K. Streicher, Nature **367**, 51 (1994).
[9] T. Palberg, H. Hecht, E. Simnacher, T. Loga, F. Falcoz, J. Kottal, and P. Leiderer, J. Phys. III (France) **4**, 457 (1994).
[10] A. P. Gast and Y. Monovoukas, Nature **351**, 533 (1991).
[11] K. Schätzel and B. J. Ackerson, Phys. Rev. E **48**, 3766 (1993).
[12] J. K. G. Dhont, C. Smits, and H. N. W. Lekkerkerker, J. Colloid Interface Sci. **152**, 386 (1992).
[13] See, for example, W. Härtl, R. Klemp, and H. Versmold, in Ref. 4, p. 229; or J. W. Aastuen, N. A. Clark, J. C. Swindal, and C. D. Muzny, in Ref. 4, p. 139.
[14] J. Liu, D. A. Weitz, and B. J. Ackerson, Phys. Rev. E **48**, 1106 (1993).
[15] B. J. Ackerson, Physica A **128**, 221 (1983).
[16] D. A. Weitz, W. D. Dozier, and P. M. Chaikin, in Ref. 2, p. 257.
[17] T. Palberg, M. Würth, R. Simon, F. Bitzer, and P. Leiderer, Prog. Colloid Polym Sci. **96**, 62 (1994).
[18] R. Piazza and V. Degiorgio, Physica A **182**, 576 (1992).
[19] T. Palberg, R. Piazza, T. Bellini, L. Belloni, W. Mönch, and F. Bitzer, Helv. Phys. Acta **67**, 225 (1994); T. Palberg, R. Piazza, T. Bellini, W. Mönch, and F. Bitzer, Phys. Rev. Lett. (submitted).
[20] T. Palberg, W. Härtl, U. Wittig, H. Versmold, M. Würth, and E. Simnacher, J. Phys. Chem. **96**, 8180 (1992).
[21] M. Deggelmann, T. Palberg, M. Hagenbüchle, E. E. Maier, R. Krause, Ch. Graf, and R. Weber, J. Colloid Interface Sci. **143**, 318 (1991).
[22] T. Palberg, J. Schwarz, and P. Leiderer, Phys. Rev. E (to be published).
[23] L. B. Chen, M. K. Chow, B. J. Ackerson, and C. F. Zukoski, Langmuir **10**, 2817 (1994).
[24] R. L. Hoffman, Trans. Soc. Rheol. **16**, 155 (1972).
[25] H. Versmold and P. Lindner, Langmuir **10**, 3043 (1994).
[26] M. J. Stevens, M. O. Robbins, and J. F. Belak, Phys. Rev. Lett. **66**, 3004 (1991).
[27] A. Imhof, A. van Blaaderen, and J. K. G. Dhont, Langmuir **10**, 3477 (1994).
[28] K. Schätzel, W. Wiese, A. Sobotta, and M. Drewel, J. Colloid Interface Sci. **143**, 287 (1991).